

ND-A187 554

LOCAL STOICHIOMETRY AND ATOMIC INTERDIFFUSION DURING
REACTIVE METAL/MERCU (U) MINNESOTAUNIV MINNEPPOLIS
DEPT OF CHEMICAL ENGINEERING AND M A WALL ET AL

1/1

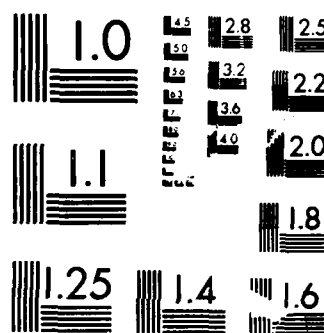
UNCLASSIFIED

23 OCT 87 TR-12 N00814-84-K-0545

F/G 7/2

NL





MICROCOPY RESOLUTION TEST CHART
NATIONAL BUREAU OF STANDARDS-1963-A

AD-A187 554

DTIC FILE COPY

LOCAL STOICHIOMETRY AND ATOMIC INTERDIFFUSION DURING REACTIVE METAL/
MERCURY-CADMIUM-TELLURIDE JUNCTION FORMATION

A. Wall, A. Raisanen, S. Chang, P. Philip, N. Troullier and A. Franciosi

Department of Chemical Engineering and Materials Science
University of Minnesota, Minneapolis, Minnesota 55455

D.J. Peterman

McDonnell Douglas Research Laboratories
St. Louis, Missouri 63166

Abstract

We summarize synchrotron radiation photoemission studies of Ag, Ge and Sm overayers on $Hg_{1-x}Cd_xTe$ (110) surfaces. These metals exhibit widely different interface reactivity with $Hg_{1-x}Cd_xTe$ and yield a range of different interface morphologies. To assess the relative importance of the microscopic driving forces that determine the local composition at the interface and in the semiconductor near surface region we present a systematic comparison of our data with calculated thermodynamic parameters such as the cation-metal heat of solution, the heat of alloying from Miedema's semiempirical model, and the metal-telluride formation enthalpy.

(Mercury-Cadmium
Cadmium Telluride)

DTIC
ELECTED
NOV 17 1987
S D
H

DISTRIBUTION STATEMENT A

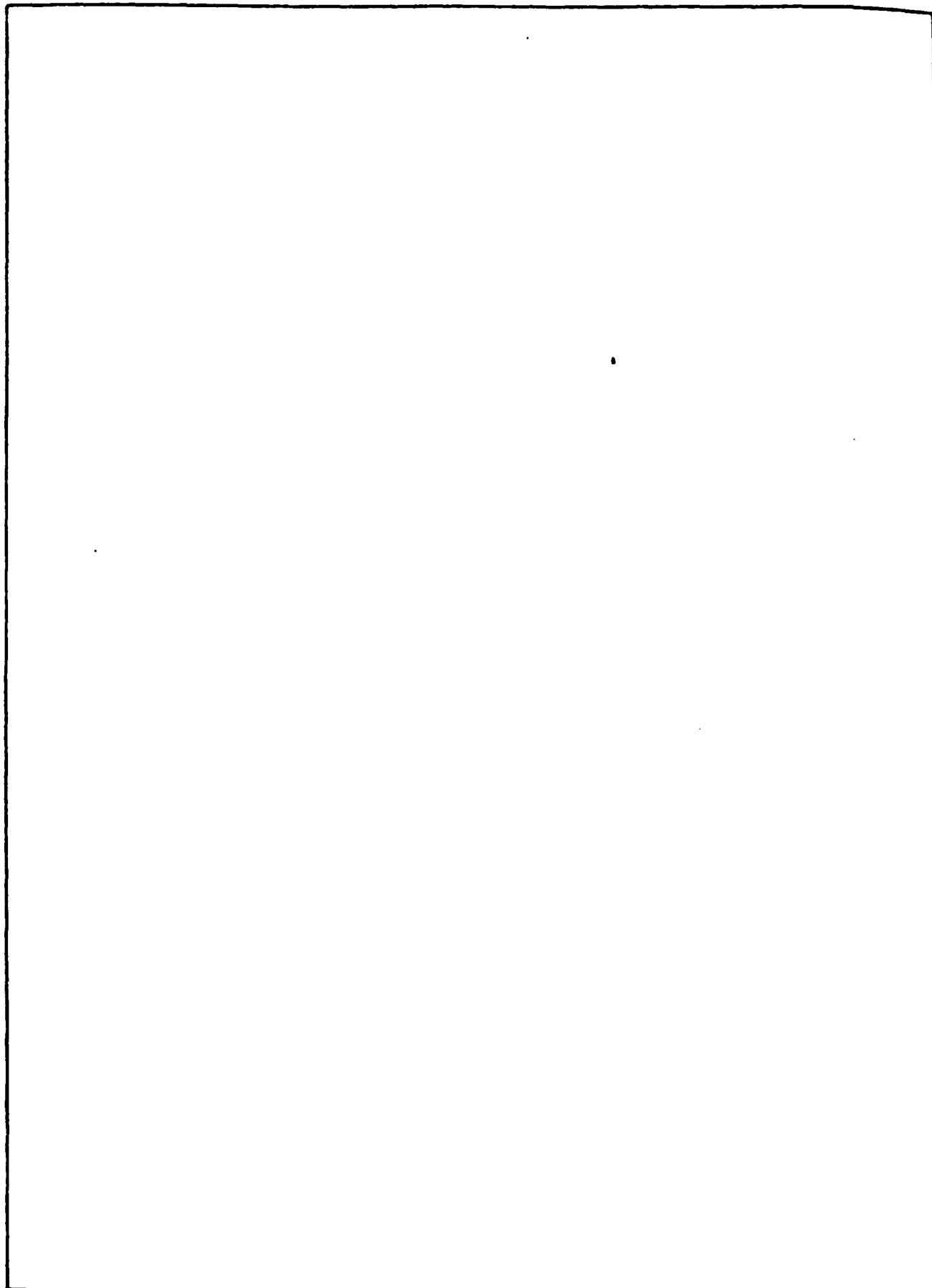
Approved for public release;
Distribution Unlimited

87 10 00 049

A/11 534

REPORT DOCUMENTATION PAGE		READ INSTRUCTIONS BEFORE COMPLETING FORM
1. REPORT NUMBER 12	2. GOVT ACCESSION NO.	3. RECIPIENT'S CATALOG NUMBER
4. TITLE (and Subtitle) LOCAL STOICHIOMETRY AND ATOMIC INTERDIFFUSION DURING REACTIVE METAL/MERCURY-CADMUM-TELLURIDE JUNCTION FORMATION		5. TYPE OF REPORT & PERIOD COVERED Interim, 8/1/86-8/31/88
7. AUTHOR(s) A. Wall, A. Raisanen, S. Chang, P. Philip, N. Troullier, A. Franciosi, and D.J. Peterman (McDonnell Douglas)		6. PERFORMING ORG. REPORT NUMBER
9. PERFORMING ORGANIZATION NAME AND ADDRESS University of Minnesota 1919 University Ave St. Paul, MN 55104		8. CONTRACT OR GRANT NUMBER(s) N00014-84-K-0545
11. CONTROLLING OFFICE NAME AND ADDRESS Dr. K. Hathaway Office of Naval Research, Electronics Division Department of the Navy		10. PROGRAM ELEMENT, PROJECT, TASK AREA & WORK UNIT NUMBERS Task NR 372-162
14. MONITORING AGENCY NAME & ADDRESS (if different from Controlling Office)		12. REPORT DATE 10/23/87
		13. NUMBER OF PAGES 18
		15. SECURITY CLASS. (of this report) unclassified
		15a. DECLASSIFICATION/DOWNGRADING SCHEDULE
16. DISTRIBUTION STATEMENT (of this Report) Approved for public release. Unlimited distribution		
17. DISTRIBUTION STATEMENT (of the abstract entered in Block 20, if different from Report)		
18. SUPPLEMENTARY NOTES To be published in J. Vac. Sci. Technol. A		
19. KEY WORDS (Continue on reverse side if necessary and identify by block number) Interface reactivity. Metal-semiconductor interfaces.		
20. ABSTRACT (Continue on reverse side if necessary and identify by block number) Ag, Ge and Sm overlayers on Mercury-Cadmium-Telluride surfaces exhibit widely different interface reactivity and yield a different range of interface morphologies. We present a systematic comparison of our synchrotron radiation photoemission results with calculated thermodynamic parameters such as the cation-metal heat of solution, the heat of alloying from Miedema's semiempirical model, and the metal-telluride formation enthalpy.		

SECURITY CLASSIFICATION OF THIS PAGE (When Data Entered)



SECURITY CLASSIFICATION OF THIS PAGE (When Data Entered)

Introduction

Although a number of promising alternate infrared materials such as $Hg_{1-x}Zn_xTe$ are attracting increasing attention¹⁻², mercury-cadmium-telluride alloys (MCT) remain the primary infrared detector material for applications in the 8-14 μm spectral range. Theoretical and experimental studies³⁻⁸ have clarified the origin of the bulk surface and interface instabilities that plague these materials, namely the competition of metallicity and ionicity in the two kinds of chemical bonds present, but controlling these instabilities is a more difficult task. The interface chemistry of MCT with metals reflects the peculiar character of the bonding in these II-VI semiconductors. For example, several authors indicate⁹⁻¹¹ that the deposition of reactive metals such as Al, In or Cr onto the MCT surface gives rise to atomic interdiffusion and to large composition gradients in the semiconductor surface layers. Since the properties of MCT are strongly composition-dependent, variations in local stoichiometry may substantially affect device performance. Reactive metal/MCT junctions of this kind generally involve a metal with relatively high telluride formation enthalpy, a substrate (MCT) with comparatively low stability, and atomic species, (Hg, Cd) with large room temperature diffusivities.

In this situation metal deposition yields a preferential overlayer-tellurium reaction, that may or may not take place via a metal/Hg exchange reaction. In general a Hg-depleted surface and near-surface layer is formed, although it is unclear at this time if the dissociated Hg migrates in the bulk or sublimes. These variations in surface composition have at times been associated with changes in the Schottky barrier¹⁰, while in other cases a connection was not found.¹¹

The phenomenological approach to the interface chemistry of MCT is now being complemented by simplified thermodynamic calculations of the different enthalpic

Availability Codes	
Dist	Avail and/or Special
A-1	

terms that drive interface reactions. For example, results for the Pt/MCT interface¹² have provided evidence that a high heat of Pt/Cd alloying may lead to a "reactive" interface even when the heat of overlayer-telluride formation is small. Atomic interdiffusion at the interface and the formation of a Hg depleted surface layer are here the results of overlayer-cation alloying rather than telluride formation.

In this paper we summarize results for three different overlayers: the supposedly unreactive Ag and Ge, and the reactive Sm. Both Ag and Ge exhibit small standard telluride formation enthalpies¹³ ($\text{Ag}_2\text{Te} = -8.6 \text{ Kcal/mol}$; $\text{GeTe} = -11.6 \text{ Kcal/mol}$). In contrast Sm exhibits some of the highest telluride formation enthalpies ($\text{SmTe} = -74 \text{ Kcal/mol}$; $\text{Sm}_2\text{Te}_3 = -190 \text{ Kcal/mol}$), much larger, for example, than those encountered in the case of Al ($\text{Al}_2\text{Te}_3 = -76.2 \text{ Kcal/mol}$). For these elements we have also performed calculations of heats of solution from the semiempirical model of Miedema et al.¹⁴ We found that the heat of solution of Cd and Hg in the three overlayers are also markedly different. We calculated negligibly small solubilities for Cd and Hg in Ag and Ge overlayers, while metallic Sm may exhibit surprisingly large solubility for Hg together with smaller solubility for Cd. These thermodynamic estimates are compared with the interface behavior observed experimentally through in situ synchrotron radiation photoemission studies. Comparison of the different microscopic evolution of the three interfaces points out the complex interplay of the different thermodynamic driving forces and kinetic barriers that determine interface behavior. For Ag we found long range Ag indiffusion in agreement with the results of Friedman et al.⁸ For Ge we observe that at coverages at and above one monolayer a complex interface evolution is dominated by preferential Ge-Te reaction. For Sm we identified two sequential stages of interface formation. In the first stage the driving force is the telluride formation enthalpy. In the second stage it is the

Hg/Sm heat of alloying which controls interface evolution.

Experimental Procedure

Experiments were conducted on single crystals of $Hg_{0.78}Cd_{0.22}Te$ grown at McDonnell Douglas Corporation with a modified Bridgman method. The samples were p-type, with a carrier concentration of $2 \times 10^{16} \text{ cm}^{-3}$. The crystals were cleaved in the photoelectron spectrometer ($p < 1 \times 10^{10} \text{ Torr}$) and the interfaces were prepared in situ by thermal evaporation onto the (110) surface with coverage monitored by a quartz thickness monitor. Metal coverage is given in terms of the (110) surface atomic density ($1 \text{ ML} = 6.76 \times 10^{14} \text{ atoms/cm}^2$, which corresponds to 1.16 \AA of metallic Ag, 2.24 \AA of Sm, and 1.53 \AA of Ge). Synchrotron radiation in the $40 \text{ eV} < h\nu < 150 \text{ eV}$ photon energy range was used to obtain angular integrated photoelectron energy distribution curves (EDC's). The radiation from the 240MeV and 1GeV electron storage rings at the Synchrotron Radiation Center of the University of Wisconsin-Madison was monochromatized with a grasshopper monochromator so that the typical overall energy resolution (electrons and photons) was of 0.2-0.4 eV. EDC's for the valence band and the Hg 5d, Cd 4d, Te 4d, Ge 3d and Ag 4d were recorded as a function of metal coverage to monitor interface evolution. In this letter we will only describe the results of such an analysis. Far more detail can be found in longer forthcoming papers that will examine separately the three overlayer systems.^{11,15-16}

Results and Discussion

In table 1 we list the relevant thermodynamic parameters for a number of metal/MCT systems. We show (left to right by column) the metal atom involved, Pauling's electronegativity, the most stable metal-tellurides in the bulk binary phase diagram¹⁴, the corresponding formation enthalpies from ref. 13, the heats of alloying of a 50/50 mixture of metal/Cd and metal/Hg, and the heats of solutions of isolated Cd and Hg atoms in the metal. The data in the four

rightmost columns were calculated¹¹ as described in refs. ^{8,11-12,14-16} following the semiempirical model of Miedema et al.¹⁴ The model describes the properties of intermetallics in terms of parameters such as the charge density at the Wigner-Seitz cell boundaries for each component and charge transfer between cells of the constituents, and tries to connect these parameters to macroscopic quantities such as the work function, compressibilities, etc. One should expect from such a simplistic picture only order-of-magnitude estimates of the thermodynamic parameters.

The data in Table 1 indicate that Ag exhibits telluride formation enthalpy even smaller than that of HgTe, such that one should assume telluride formation to be unlikely. For Ge, although the telluride formation enthalpy is small, it is larger than that of HgTe. Sm exhibits some of the highest telluride formation enthalpies encountered in the periodic table (-74 and -63 Kcal/mole Te atoms for the compounds involving divalent and trivalent Sm, respectively). The heats of the solution and alloying for cations are also markedly different. We find negligibly small solubilities for Cd and Hg in Ag or Ge. For Sm, instead, the solubility for Hg, and to a lesser extent for Cd, is expected to be relatively large. For example, the heat of solution of Hg in Sm is over 40 Kcal/mole of Sm, to be compared with a SmTe formation enthalpy of 74 Kcal/mole.

Representative EDC's for the valence and core emission from the three interfaces are shown in fig. 1. In the bottom-most section we show the emission from the $Hg_{1-x}Cd_xTe$ (110) surface, while spectra displaced upward show the effect of deposition of Ag (left), Ge (center) and Sm (right). Structure in the 7-12 eV energy range corresponds to emission from the Hg 5d doublet and from the Cd 4d cores partly superimposed on the Hg 5d_{3/2} component.

In the top left section of fig. 1 the effect of Ag deposition is seen as a slow increase with coverage of the emission from the Ag 4d states and a slow

alteration of the substrate features. Even at the highest coverages (90 monolayers) emission from Cd and Te levels is clearly visible at constant binding energy. Our results are in agreement with earlier work by Friedman et al.⁸ who proposed that Ag diffuses relatively deep in the semiconductor lattice with no preferential Ag-cation reaction or telluride formation.

The situation is completely different in the case of Ge for which we observe a complex multi-stage interface at coverages above one monolayer. In the top center section of fig. 1 there is clearly visible, for example, a nonmonotonic change of the Hg 5d to Cd 4d core intensity ratio with coverage, which reaches a minimum at a coverage of about two monolayers and increases again at higher coverages.

The coverage-dependence of the Hg 5d emission (peak intensity of the $5d_{5/2}$ component relative to the background) for Ge and Ag overayers is compared in fig. 2 with the results for Cr overayers. Cr was shown¹⁰ to react with MCT for $\theta < 2$ and give rise to a Hg-depleted surface layer through a one-to-one Cr/Hg exchange reaction. We also show in fig. 2 (shaded area) the range of attenuation expected for layer-by-layer coverage of an unreactive interface. The data for Ge are compellingly similar to those for Cr, while the indiffusion of Ag gives rise to a much slower attenuation of the Hg signal.

Analysis of the core level binding energies supports the interpretation of a direct Ge-Te reaction at the interface, that is consistent with the thermodynamic trends of Table 1. Deconvolution of the Te 4d lineshape¹⁶ shows the emergence of a high binding energy 4d doublet shifted 0.2 eV to higher binding energy. The evolution of the Ge 3d core level with coverage is shown in fig. 3. Large changes in lineshape are observed because of the emergence of low-binding energy Ge 3d features with increasing coverage.¹⁶ The center-of-mass of the 3d lineshape shifts to lower binding energy with increasing coverage and tends to

the elemental value only at the highest coverages explored. In fig. 4 we plot the binding energies of the Te 4d and Ge 3d core levels as a function of coverage. The observed relative chemical shift is substantial (-1.0 eV) and suggests that in the case of Ge at coverages at and above one monolayer Ge-Te reacted species are formed at the interface¹⁶. The submonolayer coverage range was studied earlier by Davis et al. who found little evidence of interface reaction. The effect of Sm deposition onto the MCT surface is shown in the top right section of fig. 1. Sm emission gives rise to well defined 4f final state multiplets that can be used as a fingerprint of the valence of the Sm atoms. In the early stages of interface formation divalent Sm 4f features emerge within 3eV of the Fermi level, the Hg 5d emission is quickly attenuated and the Cd to Hg ratio increases with coverage. At the highest coverages in fig. 1 emission from the Hg 5d cores is visible again, partly superimposed with the trivalent Sm 4f multiplet. The situation is shown more clearly in fig. 5¹¹ where we show a wider series of coverages (coverages are given in Å, with 1ML = 2.24Å) and an energy range that includes the Sm 5p core emission in the 17-27 eV energy range. In the top section of the figure ($\theta = 50\text{\AA}$) vertical bars mark the position of the Hg 5d core contribution and the two Sm 4f final state multiplets.

In the early stage of interface formation (below 6Å) the interaction of divalent Sm with Te which is thermodynamically favored (table 1) yields the formation of a Hg-depleted surface layer, the emergence¹¹ of a new Te 4d doublet shifted 0.4-0.5 eV, and a rigid shift to high binding energy of the Hg and Cd core levels that might be related to a 0.1-0.3 eV increase in band bending or surface bandgap.¹¹

The initial state of Sm/MCT interface formation is followed by a sharp transition to a second state ($\theta > 7\text{\AA}$) in which the Hg emission increases, and saturates at about 20% of the initial surface value.¹¹ In this coverage range,

trivalent Sm features are visible in the valence and core emission. The Sm³⁺ 4f multiplet is clearly visible in the 5-10 eV binding energy range, and the lineshape of the Sm 5p cores evolves toward that characteristic of mixed valent Sm.¹¹ The data of fig. 5, together with the coverage dependence of the core intensity and binding energies¹¹ suggest that the increase in Hg concentration is related to the formation of Sm-rich metallic phases with high solubility for Hg. This interpretation is supported by the thermodynamic trends in table 1 and by the evidence of large room temperature mobility of Hg (and Cd) relative to Te in the MCT matrix⁴⁻⁵. Incidentally, we note that this nonmonotonic behavior of the local stoichiometry with coverage is quite unprecedented, to our knowledge, in metal/semiconductor interface studies.

In this connection, we mention that we have conducted¹⁵ studies of the Te 4d emission at variable escape depth ($h\nu$ =110 and 57 eV) in order to ascertain the presence of a surface-segregated Te-rich layer for $Hg_{1-x}Cd_xTe-Sm$ at high metal coverage. Such a layer was observed during interface formation involving Al⁷ and Cr¹¹. Within experimental uncertainty we found no Te surface segregation, so that the observed Te emission reflects the actual composition of the interface reaction products¹⁵.

Conclusions

A general consideration coming from this work is that the rough estimates of the thermodynamic parameters derived from Miedema's model are surprisingly useful in understanding the thermodynamic driving forces that determine interface evolution. The case of the Sm/ $Hg_{1-x}Cd_xTe$ interface demonstrate the complex interplay of thermodynamic driving forces and kinetic "bottlenecks". At low metal coverages, when diffusion is possible for all species, the telluride formation enthalpy prevails. At high metal coverage, diffusion of Te through the reacted interface is hindered, while Hg and to a lesser extent Cd, exhibit larger

diffusion coefficients. In these conditions, the Hg/Sm heat of alloying, that is substantial even in comparison with the telluride formation enthalpy, prevails and determines the interface evolution.

To understand these systematic trends is of great importance if we want to characterize MCT interface chemistry beyond the confusing phenomenological picture constructed to date. We know which metal overlayers form interface telluride-like phases, which alloy with one or the other of the cations, and in what cases dissociated Te is released at the surface. It is comforting that we are starting to understand why. A number of problems of difficult solution remain to be addressed. For example, it is hard to see how to incorporate mass transport rate limiting processes in the semi-empirical thermodynamic picture. Along the same lines, a quantitative explanation accounting for the relatively large amounts of dissociated Te released during reaction with Sm, Al, Cr and Pt is still missing. Finally, and more importantly, it is in our opinion still debatable which compositional and structural parameters, if any, affect the Schottky barrier for MCT. A number of quite challenging questions remain for the future.

Acknowledgements

This work was supported in part by the Graduate School of the University of Minnesota, by the Office of Naval Research under contract No.0014-84-K-0545, by the Minnesota Microelectronics and Information Sciences Center, and by McDonnell Douglas Independent Research and Development Program. We thank J.H. Hollister, B.J. Morris and C.S. Wright for assistance in sample preparation, G.D. Davis for communicating his results prior to publication, and D.J. Friedman for useful discussions. We acknowledge the enthusiastic support of the staff of the University of Wisconsin Synchrotron Radiation Center, supported by the NSF.

References

- 1) J.K. Furdyna, *J. Appl. Phys.* 53, 7637 (1982) and *Proc. Int. Soc. Opt. Eng.* 409, 43 (1983).
- 2) T. Tung, M.H. Kalisher, and S. Sen, presented at the 1985 U.S. Workshop on the Physics and Chemistry of Mercury-Cadmium-Telluride.
- 3) W.A. Harrison, *J. Vac. Sci. Technol. A1*, 1672 (1983).
- 4) A.-B. Chen, A. Sher, and W.E. Spicer, *J. Vac. Sci. Technol. A1*, 1675 (1983).
- 5) W.E. Spicer, J.A. Silberman, I. Lindau, A.-B. Chen, A. Sher, and J.A. Wilson, *J. Vac. Sci. Technol. A1*, 1735 (1983) and *Phys. Rev. Lett.* 49, 948 (1982).
- 6) A. Lastras-Martinez, U. Lee, J. Zehnder, and P.M. Raccah, *J. Vac. Sci. Technol.* 21, 157 (1982).
- 7) R.R. Daniels, G. Margaritondo, G.D. Davis, and N.E. Byer, *Appl. Phys. Lett.* 42, 50 (1983).
- 8) D.J. Friedman, G.P. Carey, C.K. Shih, I. Lindau, W.E. Spicer, and J.A. Wilson, *J. Vac. Sci. Technol. A4*, 1977 (1986); J. Nogami, T. Kendelewicz, I. Lindau and W.E. Spicer, *Phys. Rev. B* 34, 669 (1986) and references therein.
- 9) G.D. Davis, N.E. Byer, R.A. Riedel, and G. Margaritondo, *J. Appl. Phys.* 57, 1915 (1982); G.D. Davis, *Il Vuoto* (Italy), to be published.
- 10) A. Raisanen, A. Wall, S. Chang, P. Philip, N. Troullier, A. Franciosi, and D.J. Peterman, *Phys. Rev. B* (in press).
- 11) A. Franciosi, P. Philip, and D.J. Peterman, *Phys. Rev.* 32, 8100 (1985); D.J. Peterman and Franciosi, *Appl. Phys. Lett.* 45, 1305 (1986).
- 12) D.J. Friedman, G.P. Carey, I. Lindau, and W.E. Spicer, *Phys. Rev. B* 35, 1188 (1987).
- 13) K.C. Mills, Thermodynamic Data for Inorganic Sulphides, Selenides, and Tellurides, Butterworths, London, 1974.
- 14) A.R. Miedema, P.F. de Chatel, and F.R. Boer, *Physica B* 100, 1 (1980).
- 15) A. Wall, A. Raisanen, S. Chang, P. Philip, A. Rizzi, A. Franciosi, and D.J. Peterman, to be published.
- 16) Decomposition of the Ge and Te core lineshape in terms of reacted components will be presented in a longer paper: A. Wall, A. Raisanen, S. Chang, P. Philip, C. Caprile, A. Franciosi and D.J. Peterman, to be published.

Table Captions

Table 1 Thermodynamic parameters calculated from the semiempirical model of Miedema et al.¹⁴ following the procedure described in refs. 11 and 12. Column 1: metal atom. Column 2: Pauling's electronegativity. Column 3: most stable metal-telluride solid phases, from ref. 13. Column 4: metal-telluride formation enthalpies, from ref. 13. Columns 5 and 6: heat of alloying (50/50 alloy) for Cd and Hg in the overlayer, respectively. Columns 7 and 8: heats of solution for isolated Cd and Hg atoms in the overlayer.

Figure Captions

Fig. 1 Bottom: Representative, photoelectron energy distribution curves (EDC's) for the valence band and core emission from the $Hg_{1-x}Cd_xTe$ (110) surface. Top: Modification of the valence states and of the shallow Cd 4d and Hg 5d core levels as a result of deposition of Ag (left), Ge (center) and Sm (right).

Fig. 2 Attenuation of the Hg core emission as a function of coverage of Ag, Ge and Cr onto the $Hg_{1-x}Cd_xTe$ (110) surface. The shaded band represents the range of attenuation expected for layer-by-layer coverage of an unreactive interface. Note the similarity of the results for Cr and Ge, and the slow attenuation observed in the case of Ag because of long range indiffusion.

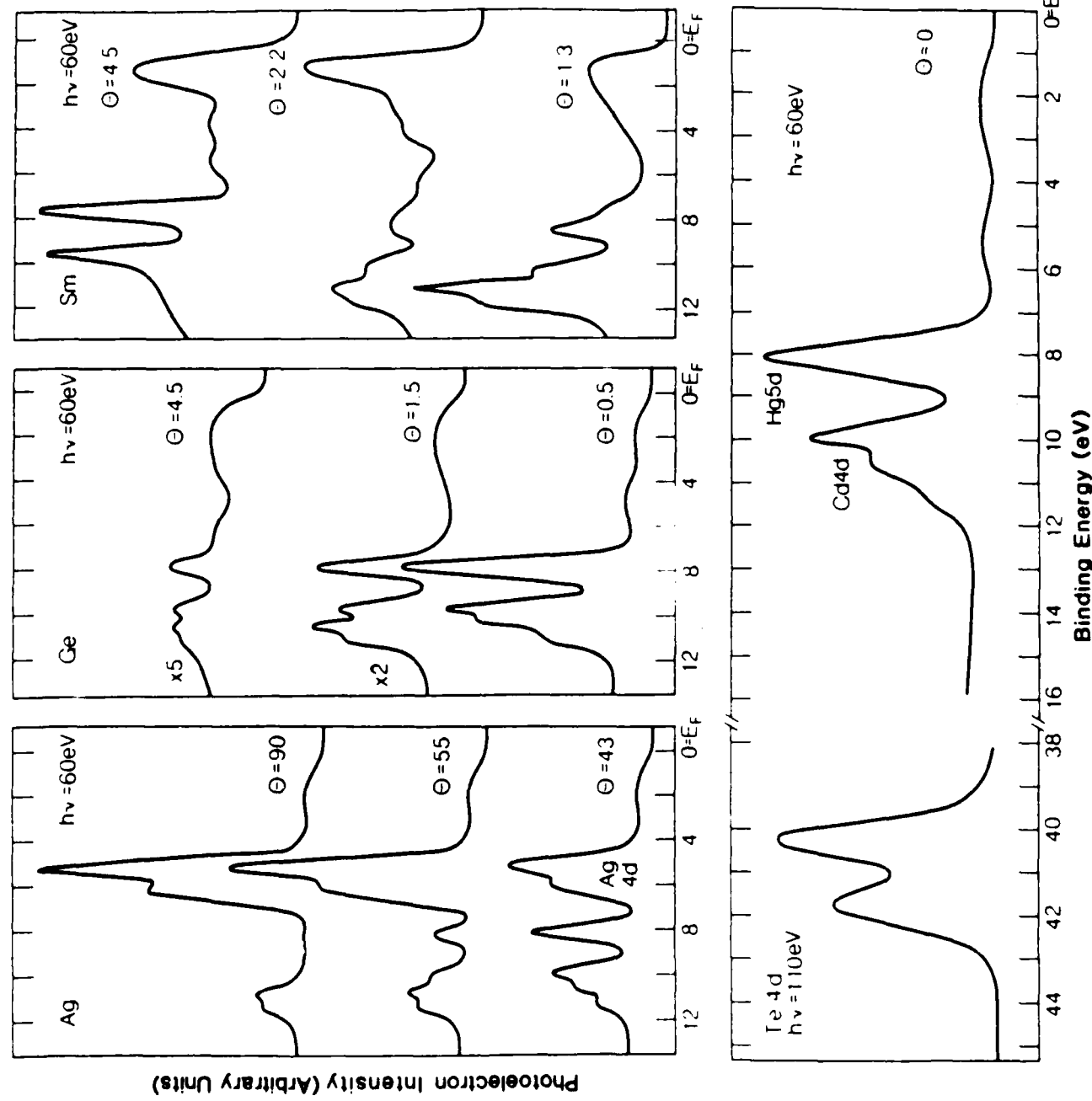
Fig. 3 EDC's for the Ge 3d core emission from the Ge/ $Hg_{1-x}Cd_xTe$ interface as a function of coverage. Large changes in lineshape are observed because of the emergence of low-binding energy Ge 3d features. At low coverage most Ge atoms interact preferentially with Te. The binding energy of the Ge cores tends to the elemental value only at the highest coverage explored.

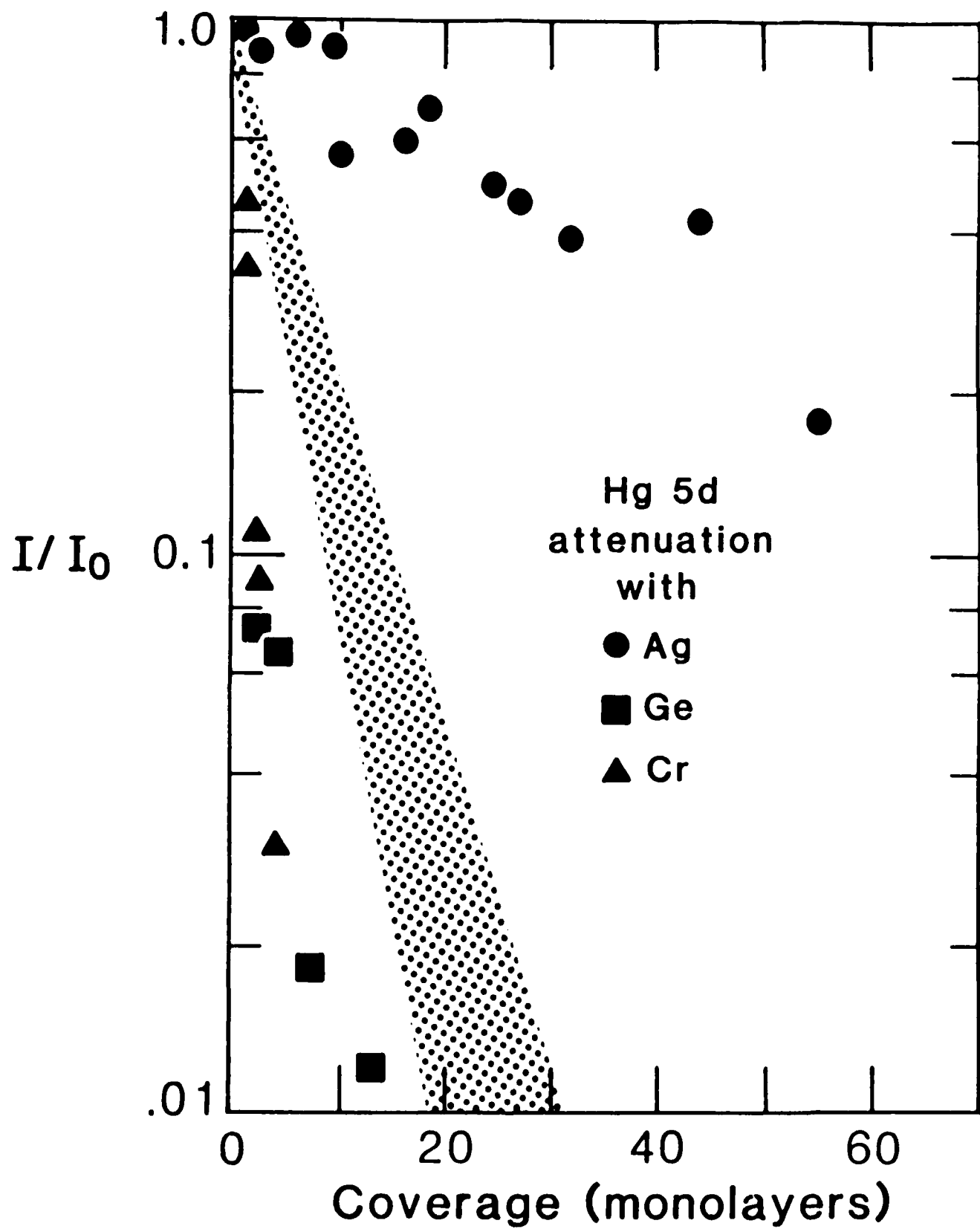
Fig. 4 Chemical shifts of the Te 4d and Ge 4d core levels from the Ge/ $Hg_{1-x}Cd_xTe$ interface as a function of coverage.

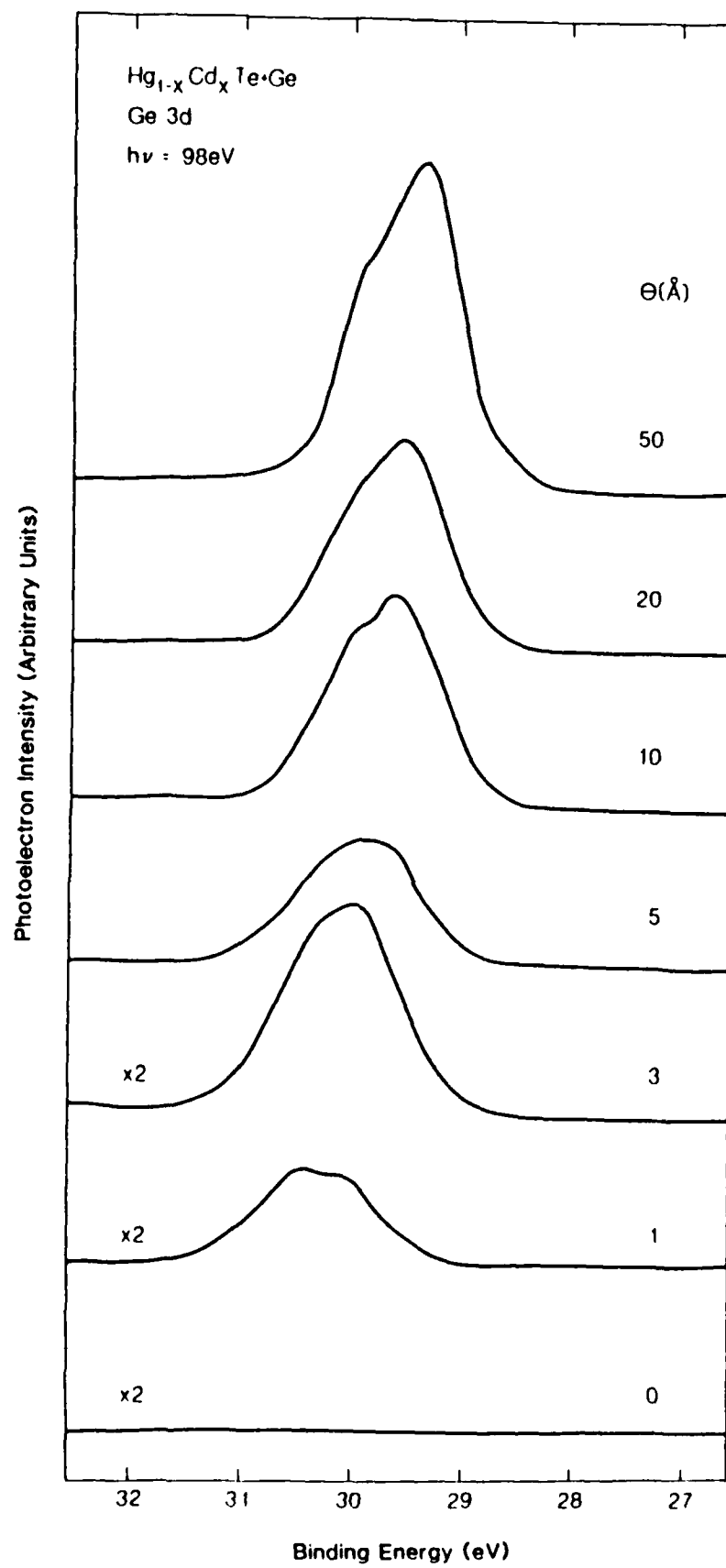
Fig. 5 Valence band emission from the $\text{Sm}/\text{Hg}_{1-x}\text{Cd}_x\text{Te}$ interface as a function of coverage in Å (1ML = 2.24Å). In the top section of the figure ($\theta = 50\text{\AA}$) we have labeled the Hg 5d core contribution and the two Sm 4f final state multiplets corresponding to divalent and trivalent Sm atoms. Features in the 17-27 eV range correspond to the Sm 5p core emission. Note the decrease of the emission for $0-5\text{\AA}$, followed by a sharp five-fold increase at $5 < \theta < 7\text{\AA}$.

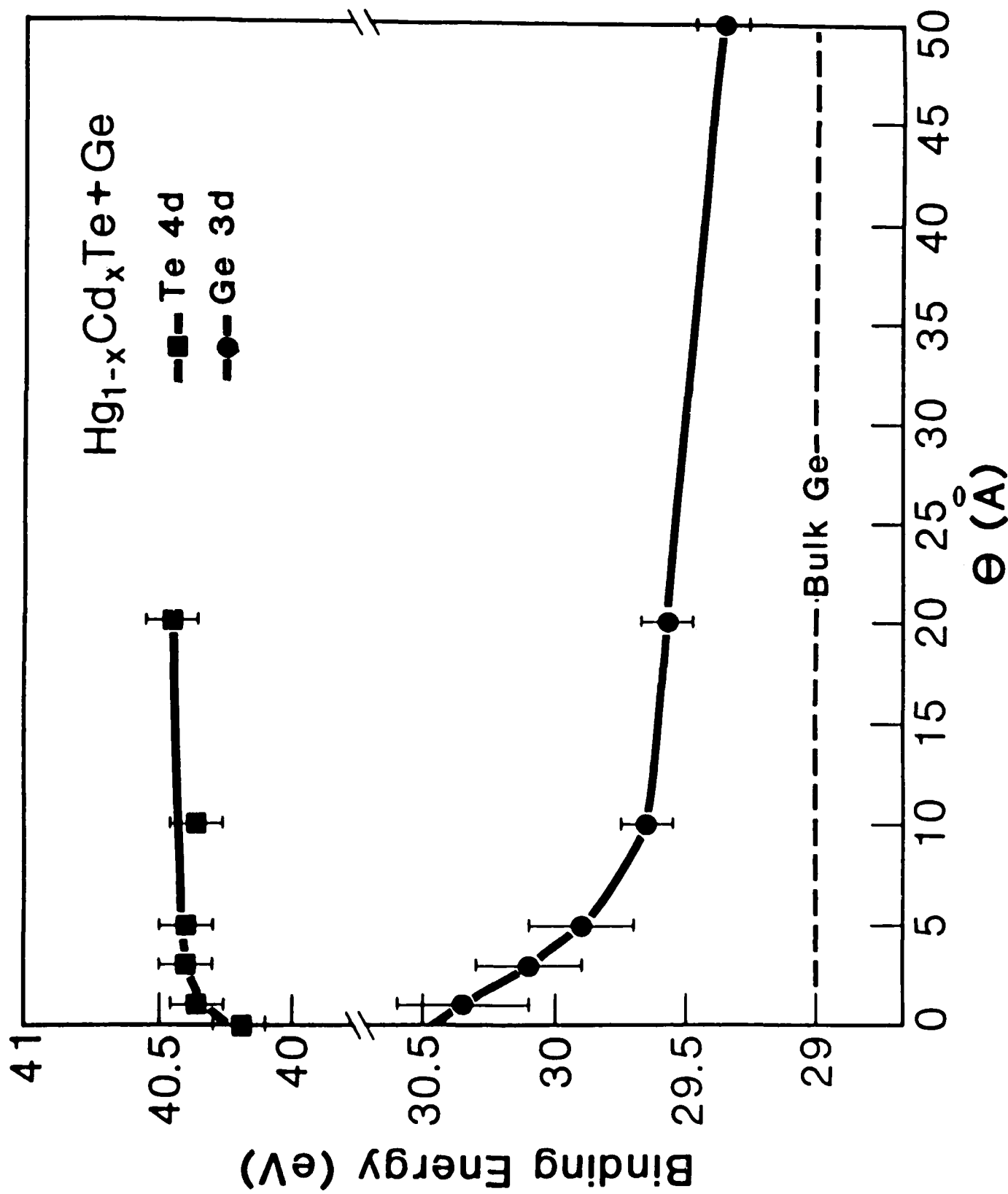
Metal (M)	electro-negativity (Pauling's)	Telluride	ΔH_f (telluride) (kcal/mol)	ΔH_f (MCd) (kcal/m)	ΔH_f (MHg) (kcal/m)	ΔH_{sol} (Cd;M) (kcal/m Cd)	ΔH_{sol} (Hg;M) (kcal/m Hg)
Cd	1.69	CdTe	-24.1	-	-	-	-
Hg	2.00	HgTe	-7.6	-	-	-	-
Ag	1.93	Ag ₂ Te	-8.6	-2.4	-1.4	-3.5	-2.2
Ge	2.01	GeTe	-11.6	+4.8	+6.4	-1.7	+0.7
Cr	1.66		-20-30	+6.9	+9.3	+11.7	+16.2
Al	1.61	Al ₂ Te ₃	-76.2	+2.4	+2.7	+3.5	+4.1
Sm ²⁺		SmTe	-74				
Sm ³⁺	1.17	Sm ₂ Te ₃	-190	-29.3	-35.3	-33.7	-41.3

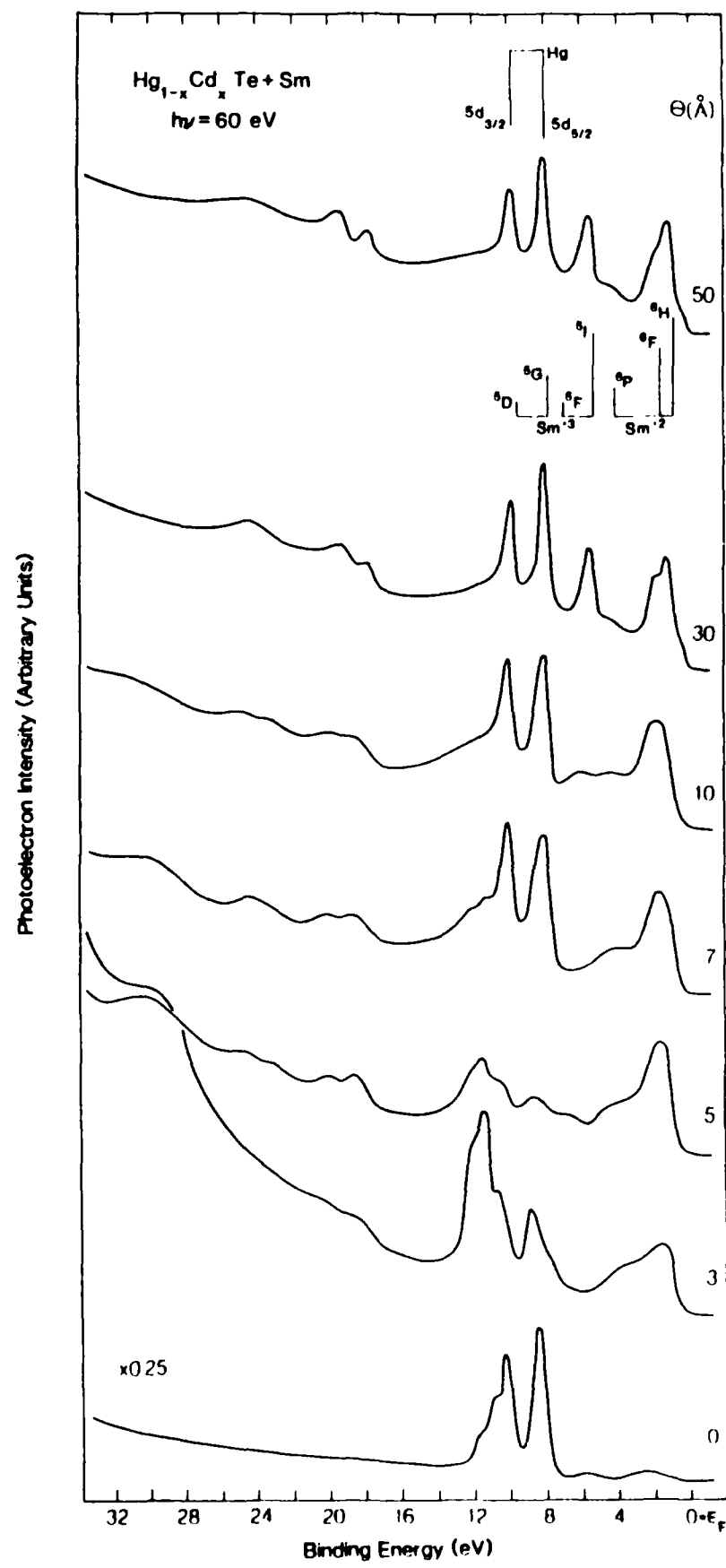
Hg_{0.9}Cd_{0.22}Te + monolayers (Θ) of:











END

FEB.

1988

DTIC